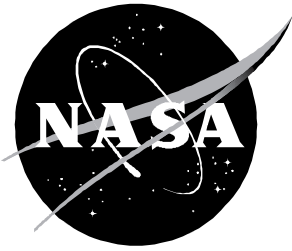


Effects of Yaw and Pitch Motion on Model Attitude Measurements

Ping Tchong, John S. Tripp, and Tom D. Finley



Effects of Yaw and Pitch Motion on Model Attitude Measurements

*Ping Tchong, John S. Tripp, and Tom D. Finley
Langley Research Center • Hampton, Virginia*

National Aeronautics and
Space Administration
Langley Research Center
Mail Code 180
Hampton, VA 23681-0001

Official Business
Penalty for Private Use, \$300

BULK RATE
POSTAGE & FEES PAID
NASA
Permit No. G-27

This publication is available from the following sources:

NASA Center for AeroSpace Information
800 Elkridge Landing Road
Linthicum Heights, MD 21090-2934
(301) 621-0390

National Technical Information Service (NTIS)
5285 Port Royal Road
Springfield, VA 22161-2171
(703) 487-4650

Abstract

This report presents a theoretical analysis of the dynamic effects of angular motion in yaw and pitch on model attitude measurements in which inertial sensors were used during wind tunnel tests. A technique is developed to reduce the error caused by these effects. The analysis shows that a 20-to-1 reduction in model attitude measurement error caused by angular motion is possible with this technique.

Introduction

The standard model attitude measurement instrumentation used at Langley Research Center (LaRC) is the inertial sensor or angle-of-attack (AOA) package described in detail in reference 1. Installed in a model during wind tunnel tests, the AOA package generates an output signal proportional to the model pitch attitude. This signal is then heavily low-pass filtered before final data processing to remove time-varying components caused by random flow noise and vibration. Certain test conditions produce oscillatory model and sting motion in pitch and yaw, which produces a centrifugal or normal acceleration component in which the average value results in constant offset errors in the sensed AOA measurement. The magnitude of the offset can be as great as 0.1° , which is unacceptable in AOA measurements in which the accuracy requirement can be as low as $\pm 0.01^\circ$. This paper presents a dynamic analysis and proposes a spectral analysis technique for detecting model and sting motion and for correcting the resulting AOA errors by a factor of 20 to 1.

Symbols

A_p	pitch oscillation amplitude, rad
A_y	yaw oscillation amplitude, rad
a_{np}	normal acceleration component caused by pitch motion, in/sec^2
a_{ny}	normal acceleration component caused by yaw motion, in/sec^2
E_p	pitch plane accelerometer
E_r	standard AOA sensor
E_y	yaw plane accelerometer
g	gravitational constant, in/sec^2
$J_n(u)$	n th-order Bessel function of first kind
r_p	pitch motion radius, in.
r_y	yaw motion radius, in.
S	AOA sensor sensitivity, V/g
t	time, sec
u	parametric constant, $\frac{A_p}{r_p}$

V_{AOA}	corrected, filtered sensor voltage output, V
V_{FFT}	power spectral line amplitude, frequency $2\phi_y$, V
V_{fil}	uncorrected, filtered sensor voltage output, V
V_{unf}	uncorrected, unfiltered sensor voltage output, V
β_p	angular pitch plane position, rad
β_y	angular yaw plane position, rad
θ	model pitch attitude, rad or deg
σ_{AOA}	standard deviation of corrected, filtered sensor output, deg
σ_{FFT}	standard deviation of power spectral line, frequency $2\phi_y$, deg
$\sigma_{\text{FFT}, i}$	standard deviation of power spectral line, i th oscillatory mode, deg
σ_{fil}	standard deviation of uncorrected, filtered sensor output, deg
ϕ_l	longitudinal oscillation frequency, rad/sec
ϕ_p	pitch plane oscillation frequency, rad/sec
ϕ_y	yaw plane oscillation frequency, rad/sec
ω_p	angular velocity in pitch, rad/sec
ω_y	angular velocity in yaw, rad/sec
Abbreviations:	
AOA	angle of attack
FFT	fast-Fourier transform

Analysis of Yaw and Pitch Motion

As shown in figure 1, let β_p and β_y denote the angular motion of the model in pitch and yaw, respectively. Let ϕ_p and ϕ_y , and A_p and A_y denote the frequencies and amplitudes of oscillation in the respective planes. Yaw and pitch will be analyzed separately.

Motion in Yaw Plane

Yaw motion is first modeled as in the following equations:

$$\left. \begin{aligned} \beta_y &= A_y \sin \phi_y t \\ \omega_y &= A_y \phi_y \cos \phi_y t \\ a_{ny} &= r_y \omega_y^2 \end{aligned} \right\} \quad (1)$$

where ω_y is the angular velocity, a_{ny} is the normal component of the acceleration vector, r_y is the radius, and t is time. Combining the second and third expressions of equations (1) yields the normal component of the acceleration vector as a function of time:

$$a_{ny}(t) = \frac{r_y A_y^2 \phi_y^2}{2} (1 + \cos 2\phi_y t) \quad (2)$$

The standard LaRC AOA package is installed in an airplane model as shown in figure 2, with its sensitive axis parallel to the longitudinal axis of the model. The AOA output signal caused by angular motion in yaw, prior to filtering, is

$$V_{\text{unf}} = S \left[g \sin \theta - \frac{r_y A_y^2 \phi_y^2}{2} (1 + \cos 2\phi_y t) \right] \quad (3)$$

where V_{unf} is the uncorrected, unfiltered sensor-package output voltage, S is the AOA sensor sensitivity, g is the gravitational constant, and θ is the model pitch attitude or angle of attack, expressed in radians for computation and converted to degrees for final presentation. The three terms of equation (3) are presented in figure 3 as functions of time. After filtering, the sensor output is the sum of the first two terms of equation (3) as shown in the following equation:

$$V_{\text{fil}} = S \left(g \sin \theta - \frac{r_y A_y^2 \phi_y^2}{2} \right) \quad (4)$$

where V_{fil} is the uncorrected, filtered sensor output. The offset error, given by the second term $r_y A_y^2 \phi_y^2 / 2$ and equal to the amplitude of the third term of equation (3), can be determined from the power spectrum of the unfiltered sensor output at frequency $2\phi_y$. Thus,

$$V_{\text{FFT}} = S \left(\frac{r_y A_y^2 \phi_y^2}{2} \right) \quad (5)$$

where V_{FFT} is the power spectral amplitude at frequency $2\phi_y$. The corrected, filtered sensor output V_{AOA} finally becomes

$$V_{\text{AOA}} = V_{\text{fil}} + V_{\text{FFT}} \quad (6)$$

Motion in Pitch Plane

Pitch motion is similarly modeled in the following equations:

$$\left. \begin{aligned} \beta_p &= A_p \sin \phi_p t \\ \omega_p &= A_p \phi_p \cos \phi_p t \\ a_{np} &= r_p \omega_p^2 \end{aligned} \right\} \quad (7)$$

where ω_p is the angular velocity, a_{np} is the normal acceleration component, r_p is the radius, and t is time. The normal acceleration component can be expressed as

$$a_{np}(t) = \frac{r_p A_p^2 \phi_p^2}{2} (1 + \cos 2\phi_p t) \quad (8)$$

If the angular pitch motion is superimposed on the pitch angle, equation (3) becomes

$$V_{\text{unf}} = S \left[g \sin \left(\theta + \frac{A_p}{r_p} \sin \phi_p t \right) - \frac{r_p A_p^2 \phi_p^2}{2} (1 + \cos 2\phi_p t) \right] \quad (9)$$

Equation (9) can be further approximated using equation (6) to yield the following:

$$V_{\text{unf}} \approx S \left[g \sin \theta + \frac{A_p g}{r_p} \cos \theta \sin \phi_p t - \frac{r_p A_p^2 \phi_p^2}{2} (1 + \cos 2\phi_p t) \right] \quad (10)$$

In addition to the normal acceleration vector component, comparison of equations (3) and (10) shows the presence of another sinusoidal component at frequency ϕ_p caused by frequency modulation. The modulation component at ϕ_p does not produce offset, and error correction is unnecessary at this frequency. Additional sensors may be required to identify these modulation frequencies. The same error correction method is used for both yaw and pitch. That is, the corrected AOA sensor output is the sum of the uncorrected filtered output and the amplitude of the spectral component at frequency $2\phi_p$.

Magnitude Estimate of Error Caused by Angular Motion

The AOA offset error, as expressed in equation (5), is presented in figure 4 as families of curves parameterized for typical values of the angular motion amplitude and its radius over frequencies from 0 to 30 Hz. Experimental AOA offset errors of 0.1° have been observed. These errors correspond to a 0.2° motion amplitude at a

30-in. radius at 10 Hz. Figure 4 illustrates curves of AOA offset errors at radii of 6 and 30 in. and at angular amplitudes from 0.1° to 0.2° . Other combinations of radius, amplitude, and frequency may produce AOA offset errors up to 0.1° .

AOA Sensor-Package Configuration

The total sensor output which results from multiple oscillatory modes is presented and shows that additional sensors are required to identify uniquely those oscillatory modes arising from angular motion. An error analysis follows that estimates the error reduction provided by the proposed technique.

AOA Sensor-Package Output

The AOA sensor-package output contains at least the following signal components:

1. Constant component $\sin\theta$ caused by model pitch angle
2. Time-varying and constant components caused by angular yaw motion
3. Time-varying and constant components caused by angular pitch motion
4. Time-varying components along the model longitudinal axis

Note that all time-varying components can be removed by low-pass filtering. Spectral analysis of the unfiltered sensor output identifies all time-varying components in the signal. Appropriate correction is applied to those components producing AOA error. Term-by-term error correction is required for multiple oscillatory modes in pitch and yaw identified by the spectral analysis.

Three-Axis Sensor Package

The proposed technique to reduce AOA error requires a spectral line estimate of the unfiltered AOA sensor-package output. However, as indicated in equation (10), indiscriminate use of fast-Fourier transform (FFT) spectral lines may result in improper correction for modulation components. Consequently, additional sensors in pitch and yaw are required to identify only those oscillatory components producing AOA errors. Figure 5 shows a proposed three-axis sensor package that consists of a standard LaRC AOA sensor E_r aligned with the model longitudinal axis and two miniature accelerometers E_y and E_p mounted in the yaw and pitch planes, respectively. Accelerometer E_y , mounted transversely to the roll axis, responds only to yaw motion. Since E_y does not respond to normal accelera-

tion produced by angular motion in either pitch or yaw, its output does not contain the constant terms or the time-varying components at frequencies $2\phi_y$ and $2\phi_p$ appearing in equations (2) and (8). Accelerometer E_y output, however, does contain the tangential acceleration component at frequency ϕ_y . Similarly, accelerometer E_p , mounted orthogonally to E_r , does not respond to normal acceleration produced by either pitch or yaw motion. It does respond to the tangential acceleration component in the pitch plane at frequency ϕ_p and to the cosine component of the gravitational vector. The presence of angular motion in each plane can thus be identified from the power spectral component frequency signatures of the three accelerometer outputs, as summarized in table I.

Table I. Sensor Power Spectral Frequency Components

Input motion	Components for accelerometer—		
	E_r	E_y	E_p
Axial	ϕ_l		
Yaw	$2\phi_y$	ϕ_y	
Pitch	$\phi_p, 2\phi_p$		ϕ_p

Of the four spectral components in the E_r power spectrum, only those modes at frequencies $2\phi_y$ and $2\phi_p$ produce AOA offset errors that require correction. Therefore, the noncontributing modes at ϕ_l and ϕ_p must be identified and discarded. The following procedure identifies those frequency components in E_r to be included or eliminated for correction of AOA offset errors.

1. Frequency ϕ_p is obtained from the cross spectrum of E_p and E_r outputs; ϕ_p is eliminated, and a correction is made at $2\phi_p$.
2. Frequency ϕ_y is obtained from the E_y power spectrum. The E_r power spectrum is searched for a component at frequency $2\phi_y$ for correction.
3. The remaining frequency components in the E_r spectrum, assumed to be longitudinal, are eliminated.

Measurement Uncertainty Estimate

The variance of AOA measurements provided by this method is obtained from the variance of equation (6):

$$\sigma_{\text{AOA}}^2 = \sigma_{\text{fil}}^2 + \sigma_{\text{FFT}}^2 \quad (11)$$

If additional oscillatory modes that contribute significantly to the total AOA error are identified, their individual error values must be included in the following form:

$$\sigma_{\text{FFT}}^2 = \sum_{i=1}^n \sigma_{\text{FFT},i}^2 \quad (12)$$

where $\sigma_{\text{FFT},i}^2$ is the measurement error variance of the i th oscillatory mode.

For a maximum AOA offset error of 0.1° and an estimated 5-percent spectral analysis accuracy, the standard deviation of the AOA offset error becomes

$$\sigma_{\text{FFT}} = 0.05 \times 0.1^\circ = 0.005^\circ \quad (13)$$

Thus, a 20-to-1 reduction in the error portion caused by angular motion is possible. Equation (11) and the assumption that $\sigma_{\text{fil}} = \pm 0.01^\circ$ (ref. 1) show that the total error is

$$\sigma_{\text{AOA}} = 0.011^\circ \quad (14)$$

Concluding Remarks

This paper is a theoretical treatment of angular motion effects upon inertially sensed model attitude measurements. A technique was developed to identify the time-varying components that produce angle-of-attack (AOA) offset errors. The analysis quantifies the offset error magnitudes, based on knowledge of the angular motion radii and frequencies. Spectral analysis techniques identify only those frequency components of the motion that contribute to AOA offset errors. A technique that does not require prior knowledge of the radius of motion is proposed to estimate AOA offset error magnitudes. Experimental verification of the proposed method has not been attempted. Note that the AOA offset error cannot be removed by filtering or time averaging.

NASA Langley Research Center
Hampton, VA 23681-0001
November 28, 1994

Appendix

Approximation of Angular Motion in Pitch

Equation (10) describes the angular pitch motion. The first term contains $\sin \theta$, and is phase modulated by the sinusoidally varying angular motion at amplitude A_p/r_p at frequency ϕ_p , as shown in the following equation:

$$f(t) = \sin(\theta + u \sin \phi_p t) \quad (\text{A1})$$

where $u = A_p/r_p$. Expand equation (A1) using trigonometric identities into the form

$$f(t) = \sin \theta \cos(u \sin \phi_p t) + \cos \theta \sin(u \sin \phi_p t) \quad (\text{A2})$$

The second factor of each term of equation (A2) can be expanded as follows:

$$\left. \begin{aligned} \cos(u \sin \phi_p t) &= J_0(u) + 2 \sum_{n=1}^{\infty} J_{2n}(u) \cos 2n \phi_p t \\ \sin(u \sin \phi_p t) &= 2 \sum_{n=1}^{\infty} J_{2n-1}(u) \sin (2n-1) \phi_p t \end{aligned} \right\} \quad (\text{A3})$$

where $J_n(u)$ is the n th-order Bessel function of the first kind. For the values of A_p and r_p , cited in figure 4, u ranges from 0.001 to 0.008, for which the Bessel functions are closely approximated as

$$\left. \begin{aligned} J_0(u) &\approx 1 \\ J_1(u) &\approx \frac{u}{2} \\ J_n(u) &\approx 0 \quad (n > 1) \end{aligned} \right\} \quad (\text{A4})$$

where $J_0(0.001) = 1.00000$, $J_0(0.008) = 0.99998$, $J_1(0.001) = 0.00050000$, $J_1(0.008) = 0.0040000$, $J_2(0.001) = 1.2 \times 10^{-7}$, $J_2(0.008) = 0.0000008$, and so on. Therefore, equations (A3) can be approximated as

$$\left. \begin{aligned} \cos(u \sin \phi t) &\approx J_0(u) \approx 1 \\ \sin(u \sin \phi t) &\approx 2J_1(u) \sin \phi t \approx u \sin \phi t \end{aligned} \right\} \quad (\text{A5})$$

Thus, function $f(t)$ in equation (A2) simplifies to

$$f(t) \approx \sin \theta + u \cos \theta \sin \phi t \quad (\text{A6})$$

Reference

1. Finley, Tom D.; and Tchong, Ping: Model Attitude Measurements at NASA Langley Research Center. AIAA-92-0763, Jan. 1992.

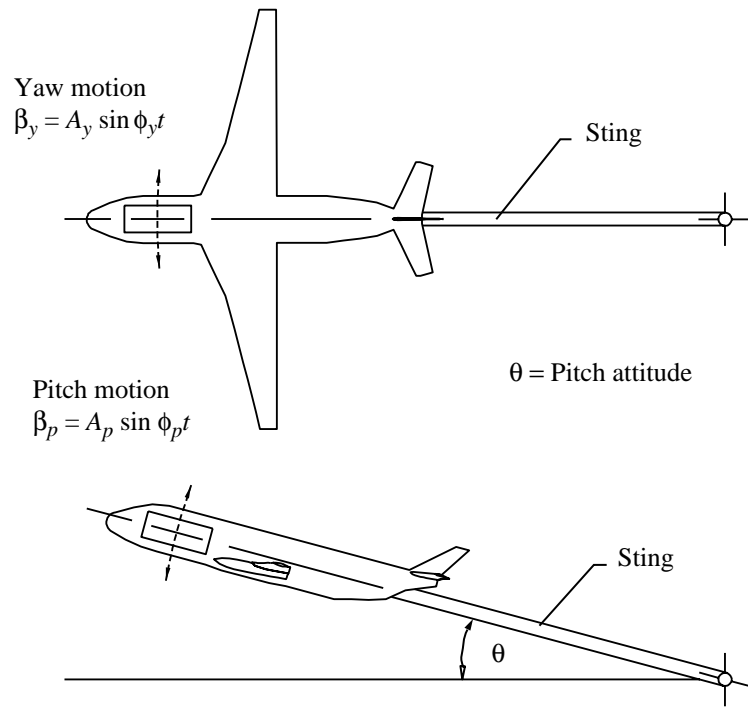


Figure 1. Yaw and pitch motion of wind tunnel model.

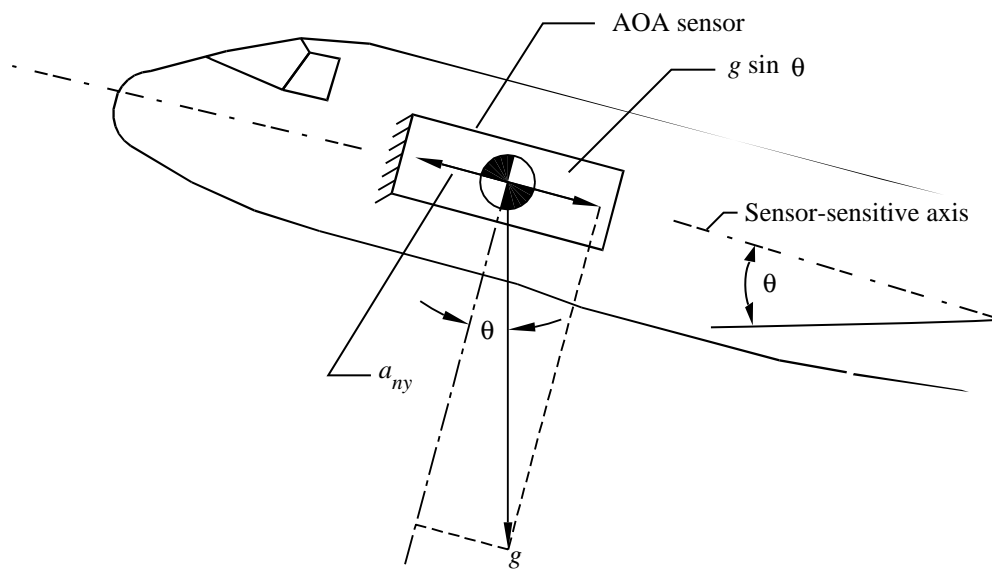


Figure 2. AOA sensor installation.

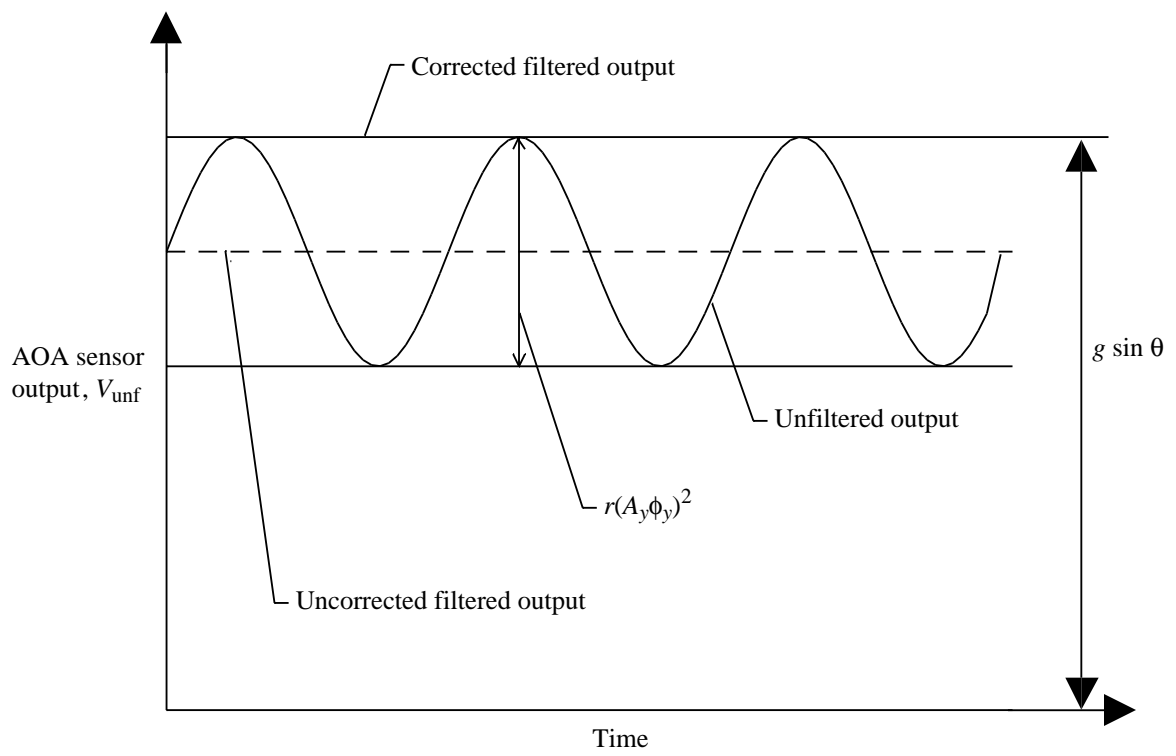


Figure 3. AOA sensor output.

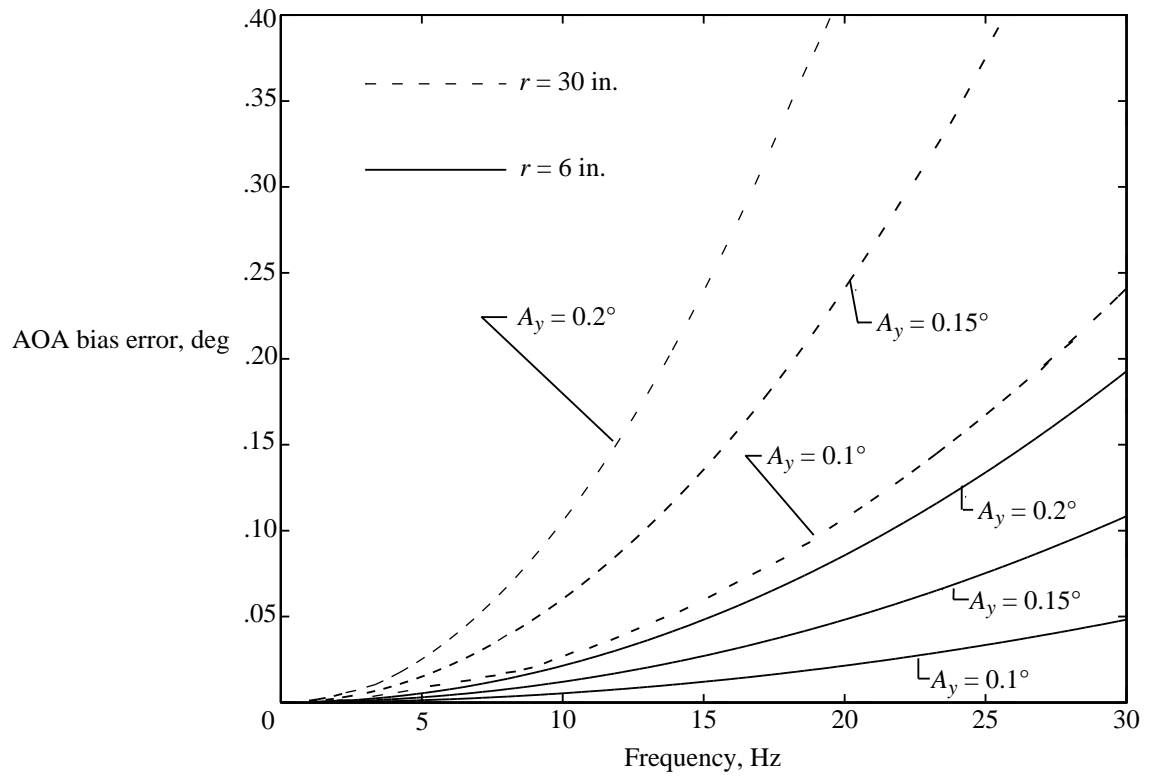


Figure 4. AOA offset error caused by model dynamics.

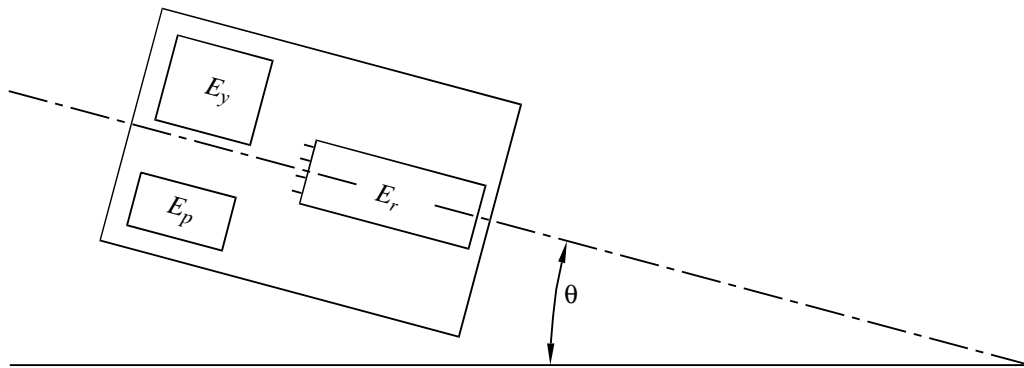


Figure 5. Three-axis AOA sensor package.

REPORT DOCUMENTATION PAGE			Form Approved OMB No. 0704-0188	
Public reporting burden for this collection of information is estimated to average 1 hour per response, including the time for reviewing instructions, searching existing data sources, gathering and maintaining the data needed, and completing and reviewing the collection of information. Send comments regarding this burden estimate or any other aspect of this collection of information, including suggestions for reducing this burden, to Washington Headquarters Services, Directorate for Information Operations and Reports, 1215 Jefferson Davis Highway, Suite 1204, Arlington, VA 22202-4302, and to the Office of Management and Budget, Paperwork Reduction Project (0704-0188), Washington, DC 20503.				
1. AGENCY USE ONLY (Leave blank)	2. REPORT DATE February 1995	3. REPORT TYPE AND DATES COVERED Technical Memorandum		
4. TITLE AND SUBTITLE Effects of Yaw and Pitch Motion on Model Attitude Measurements		5. FUNDING NUMBERS WU 505-59-54-02		
6. AUTHOR(S) Ping Tcheng, John S. Tripp, and Tom D. Finley				
7. PERFORMING ORGANIZATION NAME(S) AND ADDRESS(ES) NASA Langley Research Center Hampton, VA 23681-0001		8. PERFORMING ORGANIZATION REPORT NUMBER L-17381		
9. SPONSORING/MONITORING AGENCY NAME(S) AND ADDRESS(ES) National Aeronautics and Space Administration Washington, DC 20546-0001		10. SPONSORING/MONITORING AGENCY REPORT NUMBER NASA TM-4641		
11. SUPPLEMENTARY NOTES				
12a. DISTRIBUTION/AVAILABILITY STATEMENT Unclassified-Unlimited Subject Category 35 Availability: NASA CASI (301) 621-0390		12b. DISTRIBUTION CODE		
13. ABSTRACT (Maximum 200 words) This report presents a theoretical analysis of the dynamic effects of angular motion in yaw and pitch on model attitude measurements in which inertial sensors were used during wind tunnel tests. A technique is developed to reduce the error caused by these effects. The analysis shows that a 20-to-1 reduction in model attitude measurement error caused by angular motion is possible with this technique.				
14. SUBJECT TERMS Model attitude measurement; Inertial angle-of-attack sensors; Dynamic attitude measurements			15. NUMBER OF PAGES 9	
			16. PRICE CODE A02	
17. SECURITY CLASSIFICATION OF REPORT Unclassified	18. SECURITY CLASSIFICATION OF THIS PAGE Unclassified	19. SECURITY CLASSIFICATION OF ABSTRACT Unclassified	20. LIMITATION OF ABSTRACT	